Modeling of geometrical connection for a Hilbert bundle generated by eigenfunctions of an operator

Rudenko L.

Department of Computational Physics, St Petersburg State University

1 Introduction

Our longstanding aim is to study the three-body scattering problem. As a first step to this problem we consider a so called S-wave three body Faddeev equation and concentrate our attention on the basis, which will be used for expanding the solution [1]. We construct this basis as adiabatic harmonics when the hyperradius is considered as the adiabatic parameter. Once the basis is constructed, the standard projection procedure leads to the effective equations for the expansion coefficients. The parameters of these effective equations depend on the properties of the basis functions, particularly on the geometrical characteristics of the basis functions which are represented by the geometrical connection matrix.

Here we give a sketch of a formalism and present the behavior of eigenvalues λ_k, eigenfunctions ϕ_k, and geometrical connections $A_{ij} = \langle \phi_i, \partial_\rho \phi_j \rangle$ of the operator

$$h(\rho) = -\rho^{-2}\partial_\theta^2 + V(\rho\cos\theta).$$

This operator is generated by the simplest s-wave Faddeev differential equation (FDE) formulation of the three-body scattering problem [1].

2 Faddeev Equations in $\{\rho, \theta\}$ Coordinates

The Faddeev s-wave equation in polar coordinates has the form

$$\left(-\partial_\rho^2 - \frac{1}{4\rho^2}\right) U(\rho,\theta) + \left(-\frac{1}{\rho^2}\partial_\theta^2 + V(\rho\cos\theta)\right) U(\rho,\theta) - EU(\rho,\theta) = -V(\rho\cos\theta)\frac{\sqrt{3}}{4}\int_{\theta_-(\theta)}^{\theta_+(\theta)} d\theta'\; U(\rho,\theta'),$$

where $\theta_+(\theta) = \pi/2 - |\pi/6 - \theta|$ and $\theta_-(\theta) = |\pi/3 - \theta|$. The boundary conditions should be imposed for the scattering solution. The first set of these conditions determines the regularity of the solution

$$U(0,\theta) = U(\rho,0) = U(\rho,\pi/2) = 0. \tag{2.1}$$

The second set of conditions is the asymptotics as $\rho \to \infty$

$$U(\rho,\theta) \sim \varphi(x)\rho^{1/2}\sin(qy)/q + a(q)\varphi(x)\rho^{1/2}\exp(iqy) + A(\theta,E)\exp(i\sqrt{E}\rho), \qquad (2.2)$$

where $x = \rho\cos\theta$. The momentum of the projectile q is related to the energy E and the binding energy of the two body target ϵ by the expression

$$q^2 = E - \epsilon.$$

The bound-state wave function of the two body target system $\varphi(x)$ obeys the equation

$$\{-\partial_x^2 + V(x)\}\varphi(x) = \epsilon\,\varphi(x).$$

It is assumed that the discrete spectrum of the Hamiltonian $-\partial_x^2 + V(x)$ consists of one negative eigenvalue ϵ at most.

3 Expansion basis

We need a basis to expand the solution of the scattering problem for the Faddeev equation. As this basis we choose the eigenfunctions set of the operator $h(\rho)$

$$h(\rho)\phi_k(\theta|\rho) = \left(-\rho^{-2}\partial_\theta^2 + V(\rho\cos\theta)\right)\phi_k(\theta|\rho) = \lambda_k(\rho)\phi_k(\theta|\rho).$$

Here ρ is an external parameter for the operator $h(\rho)$. That means the eigenfunctions and the eigenvalues of $h(\rho)$ inherit parametrical dependence on ρ. The main spectral properties of the operator $h(\rho)$ as $\rho \to \infty$ and of the two body Hamiltonian $-\partial_x^2 + V(x)$ can be formulated as follows

$$\lambda = \lim_{\rho\to\infty}\lambda_0(\rho) = \epsilon,$$

$$\phi_0(\theta|\,\rho) = \sqrt{\rho}\,\varphi(\rho\cos\theta)(1 + O(\rho^{-\mu}))$$

with some $\mu > 0$. For excited states $\phi_k(\theta|\rho)$, $k \geq 1$ as $\rho \to \infty$ the asymptotic behavior is given by the formulas

$$\lambda_k(\rho) \sim \left(\frac{2k}{\rho}\right)^2,$$

$$\phi_k(\theta|\,\rho) \sim \frac{2}{\sqrt{\pi}}\sin(2k\theta).$$

4 Perturbation theory

If the parameter ρ is large, the support of the potential $V(\rho\cos\theta)$ is small on the interval $[0,\,\pi/2]$. In this case the estimates for the eigenvalues and the eigenfunctions of the operator $h(\rho)$ can be obtained by the perturbation theory considering the potential $V(\rho\cos\theta)$ as a small perturbation

$$\lambda_k \sim \lambda_k^{(0)} + \lambda_k^{(1)}, \qquad (4.3)$$

$$\phi_k(\theta|\rho) \sim \phi_k^{(0)}(\theta|\,\rho) + \phi_k^{(1)}(\theta|\,\rho). \qquad (4.4)$$

Here the leading terms $\lambda_k^{(0)}$ and $\phi_k^{(0)}$ for $k \geq 1$ are given by

$$\lambda_k^{(0)} = (2k)^2/\rho^2, \tag{4.5}$$

$$\phi_k^{(0)}(\theta|\,\rho) = \frac{2}{\sqrt{\pi}}\sin(2k\theta). \tag{4.6}$$

The first order correction terms $\lambda_k^{(1)}$ and $\phi_k^{(1)}$ are defined in terms of the matrix elements of the potential $V(\rho\cos\theta)$

$$V_{nk}(\rho) = \langle\phi_n^{(0)}|\,V|\,\phi_k^{(0)}\rangle = \int_0^{\pi/2} d\theta\,\phi_n^{(0)}(\theta|\,\rho)V(\rho\cos\theta)\phi_k^{(0)}(\theta|\,\rho). \tag{4.7}$$

As the model situation, we estimate the behavior of the matrix elements $V_{nk}(\rho)$ for large values of ρ for the special case of the function $V(x)$ taken in the form of the Yukawa potential

$$V(x) = C\,\frac{\exp(-\mu x)}{x},$$

where C and μ are some parameters.

As $\rho \to \infty$ we approximately estimate the value of the integral (4.7). The potential $V(x)$ is nonzero in the interval [0, R], where R is the large parameter. We may consider those values of θ which are obeyed the inequality $\rho\cos\theta < R$, or $\cos\theta < R/\rho$, and set the potential $V(x) = 0$ for the others values. In this case the ratio R/ρ can be considered as the small parameter for the perturbation theory. After this suggestion we consider the integral on the interval $\theta \in [\arccos(R/\rho), \pi/2] \simeq [\pi/2 - R/\rho, \pi/2]$. We get the following estimation for $V_{nk}(\rho)$ by integrating by parts

$$V_{nk}(\rho) \sim (-1)^{n+k}\frac{16nkC}{\pi}\frac{[1-\exp(-\mu R)(1+\mu R)]}{\mu^2}\frac{1}{\rho^3}.$$

The matrix element V_{nk} depends on the parameter $\rho \to \infty$ as

$$V_{nk}(\rho) \sim \rho^{-3}.$$

The first order correction term $\lambda_k^{(1)}$ is

$$\lambda_k^{(1)} = V_{kk} \sim \frac{16k^2C}{\pi}\frac{[1-\exp(-\mu R)(1+\mu R)]}{\mu^2}\frac{1}{\rho^3} \sim \rho^{-3}.$$

The second order correction term has the form

$$\lambda_k^{(2)} = \sum_{n\neq k}\frac{|V_{nk}|^2}{\lambda_k^{(0)} - \lambda_n^{(0)}},$$

which leads to the dependence

$$\lambda_k^{(2)} \sim \rho^{-4}.$$

The first correction term for the eigenfunction is given by

$$\phi_k^{(1)} = \sum_{n\neq k}\frac{V_{nk}}{\lambda_k^{(0)} - \lambda_n^{(0)}}\,\phi_n^{(0)} \sim \rho^{-1}.$$

Previously, we introduced the geometrical connections A_{ij} as $\langle \phi_i, \partial_\rho \phi_j \rangle$. From the equation

$$\left(-\rho^{-2}\,\partial_\theta^2 + V(\rho\cos\theta)\right)\phi_k(\theta|\rho) = \lambda_k(\rho)\phi_k(\theta|\rho)$$

it is easily seen that another form for A_{ij} in terms of the potential reads

$$A_{ij} = \frac{\langle \phi_i|\,\partial_\rho(\rho^2 V(\rho\cos\theta))|\,\phi_j\rangle}{\rho^2(\lambda_j - \lambda_i)}.$$

Using the above asymptotics for eigenfunctions and eigenvalues as $\rho \to \infty$ we arrive to the asymptotic behavior of the geometrical connection A_{ij}

$$A_{ij} \sim \frac{1}{\rho^2},\ i,j \neq 0, \tag{4.8}$$

$$A_{ij} \sim \frac{1}{\rho^{5/2}},\ i = 0\ or\ j = 0. \tag{4.9}$$

5 Solution expansion

The operator $h(\rho)$ is Hermitian on $[0, \pi/2]$ interval with zero boundary conditions and its eigenfunction set $\{\phi_k(\theta|\,\rho)\}_0^\infty$ is complete. This set can be used to expand the solution of the Faddeev equation as

$$U(\rho,\theta) = \phi_0(\theta|\,\rho)F_0(\rho) + \sum_{k\geq 1}\phi_k(\theta|\,\rho)F_k(\rho).$$

The asymptotic behavior of the coefficients $F_k(\rho)$ as $\rho \to \infty$ follows from (2.2) and has the form

$$F_0(\rho) \sim \sin(q\rho)/q + a_0(q)\exp(iq\rho) \tag{5.10}$$

for the elastic scattering channel, where $q^2 = E - \lambda$, $\lambda = \lim_{\rho\to\infty}\lambda_0(\rho)$. For break-up channels the correct asymptotics for $k \geq 1$ case has the form

$$F_k(\rho) \sim a_k(E)\exp(i\sqrt{E}\rho), k \geq 1. \tag{5.11}$$

The comparison of (2.2) and (5.10) and (5.11) leads to the identification

$$a(q) = a_0(q),$$

$$A(\theta, E) = \sum_{k\geq 1} a_k(E)\phi_k(\theta|\,\infty),$$

where

$$\phi_k(\theta|\,\infty) = \lim_{\rho\to\infty}\phi_k(\theta|\,\rho).$$

Introducing this expansion in the Faddev equation and projecting on basis functions lead us to the following set of equations for the coefficients $F_k(\rho), k = 0, 1, ...$

$$\left(-\partial_\rho^2 - \frac{1}{4\rho^2} + \lambda_k(\rho) - E\right)F_k(\rho) = \sum_{i=0}^{\infty}\left[2A_{ki}\frac{\partial F_i(\rho)}{\partial\rho} + B_{ki}(\rho)F_i(\rho) - W_{ki}(\rho)F_i(\rho)\right]. \tag{5.12}$$

Here the nonadiabatical matrix elements $A_{ki}(\rho), B_{ki}(\rho)$ and potential coupling matrix $W_{ki}(\rho)$ are given by integrals

$$A_{ki}(\rho) = \langle \phi_k |\, \partial_\rho\, \phi_i \rangle = \int_0^{\pi/2} d\theta\, \phi_k^*(\theta|\,\rho) \frac{\partial \phi_i(\theta|\,\rho)}{\partial \rho},$$

$$B_{ki}(\rho) = \langle \phi_k |\, \partial_\rho^2\, \phi_i \rangle = \int_0^{\pi/2} d\theta\, \phi_k^*(\theta|\,\rho) \frac{\partial^2 \phi_i(\theta|\,\rho)}{\partial \rho^2},$$

$$W_{ki}(\rho) = \frac{\sqrt{3}}{4} \int_0^{\pi/2} d\theta\, \phi_k^*(\theta|\,\rho) V(\rho\cos\theta) \int_{\theta_-(\theta)}^{\theta_+(\theta)} d\theta'\, \phi_i(\theta'|\,\rho).$$

Let us study the asymptotic behavior of functions $F_k(\rho)$ resulted from the equation (5.12). Let us consider these equations in case $\rho \to \infty$. For further investigation it is useful to change the form of the equation (5.12) to make it selfadjoint. That means excluding the term with the first derivative of F_i.

Let us transform the equation (5.12) into the matrix form. Here we introduce few matrices. $F(\rho)$ is infinite one row matrix which consists of the coefficients $F_k(\rho)$. Matrices A, B, W are infinite matrices related to the coefficients A_{ki}, B_{ki}, W_{ki} respectively. Λ is the infinite diagonal matrix, with diagonal elements $\lambda_k(\rho)$. The equation (5.12) assumes the form

$$\left(-\partial_\rho^2 - \frac{1}{4\rho^2} + \Lambda(\rho) - E \right) F(\rho) = 2A\partial_\rho F(\rho) + (B - W)F(\rho), \tag{5.13}$$

or

$$F''(\rho) + PF'(\rho) + QF(\rho) = 0, \tag{5.14}$$

were $P = 2A$ and $Q = (1/4\rho^{-2} - \Lambda(\rho) + E + B - W)$ and "prime" means the derivative over ρ.

We introduce the matrix transformation $F = UG$ and consider elements of G as new unknown quantities and choose the transformation matrix U in such a way the resulting equation for G will contain no first derivative. After substitution $F = UG$ into (5.14) we get

$$UG'' + (2U' + PU)\, G' + (U'' + PU' + QU)\, G = 0. \tag{5.15}$$

We set $2U' + PU = 0$ which leads to the matrix equation

$$U' = -\frac{1}{2} PU = -AU. \tag{5.16}$$

The solution to this equation can be given by the integral equation of the form

$$U(\rho) = I + \int_\rho^\infty AU d\rho \tag{5.17}$$

where I is the unite matrix. The integral equation is defined correctly if the integral in the right hand side converges. This will be guaranteed if the matrix A behaves as $A(\rho) \sim 1/\rho^{1+\epsilon},\ \epsilon > 0$ what is fulfilled in view of (4.8, 4.9). Hence, the asymptotics is valid

$$U \to I$$

as $\rho \to \infty$.

By using (5.16) in the equation (5.15) we get the form without first derivative F'

$$UG'' + \left(-\frac{1}{2}P' - \frac{1}{4}P^2 + Q\right)UG = 0.$$

After substitution of the expressions for P and Q we obtain the final form

$$G'' + U^{-1}\left(-A'(\rho) - A^2(\rho) + \frac{1}{4\rho^2} - \Lambda(\rho) + E + B - W\right)UG = 0. \tag{5.18}$$

As $\rho \to \infty$ we can use the asymptotics $U(\rho) \sim I + O(\rho^{-1})$ and get the following asymptotical form of (5.18)

$$\left(-\partial_\rho^2 - \frac{1}{4\rho^2}I + \Lambda(\rho) - E\right)G = \left(-A'(\rho) - A^2(\rho) + B(\rho) - W(\rho)\right)G. \tag{5.19}$$

From this equation we obtain asymptotics for the elements of G as $\rho \to \infty$. Indeed, the right hand side terms vanish for large ρ faster than ρ^{-2}. Hence this terms can be neglected. The coupling terms vanish and we get uncoupled equations of the form

$$\left(-\partial_\rho^2 - \frac{1}{4\rho^2} + \lambda_k^{as}(\rho) - E\right)G_k(\rho) = 0. \tag{5.20}$$

Here $\lambda_0^{as}(\rho) = \epsilon$ and $\lambda_k^{as}(\rho) = (2k)^2/\rho^2$ for $k \geq 1$. The solutions of these equations with the appropriate asymptotics can be expressed in terms of the Bessel (Y, J) functions and the Hankel $(H^{(1)})$ functions of the first kind as following

$$G_0(\rho) \sim \sqrt{\frac{\pi q\rho}{2}}\frac{Y_0(q\rho) + J_0(q\rho)}{\sqrt{2}q} + a_0(q)\sqrt{\frac{\pi q\rho}{2}}H_0^{(1)}(q\rho)e^{i\pi/4} \tag{5.21}$$

for the elastic scattering channel, and

$$G_k(\rho) \sim a_k(E)\sqrt{\frac{\pi\sqrt{E}\rho}{2}}H_{2k}^{(1)}(\sqrt{E}\rho)e^{i(\pi/4+k\pi)} \tag{5.22}$$

for break-up channels. As the result the solution of scattering problem consists in solving equations (5.12) with asymptotics (5.21) and (5.22) as boundary conditions as $\rho \to \infty$.

6 Malfliet-Tjon potential

For numerical calculation we choose a potential, which describes the modeling nucleon-nucleon interaction acting in the triplet state with the spin 3/2. The potential has the form of the Yukawa terms superposition

$$V(x) = V_1\frac{\exp(-\mu_1 x)}{x} + V_2\frac{\exp(-\mu_2 x)}{x} \tag{6.23}$$

with parameters listed in the table:

Coefficient	Value
V_1	$-626,885\text{MeV}$
V_2	$1438,72\text{MeV}$
μ_1	$1,55\ \text{Fm}^{-1}$
μ_2	$3,11\ \text{Fm}^{-1}$

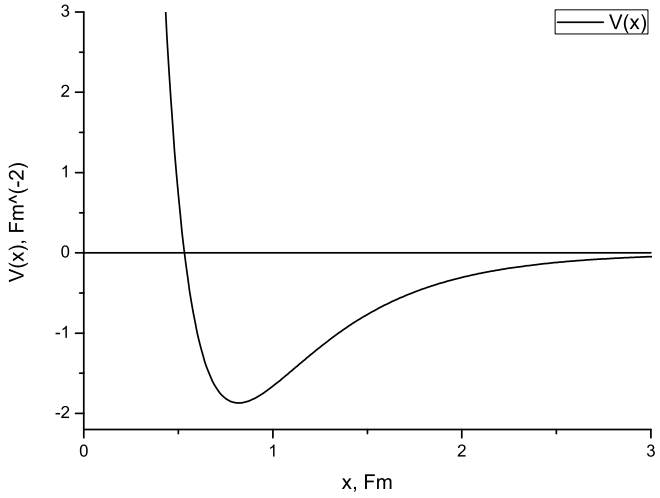

Figure 1. The Malfliet-Tjon potential

For calculations we have to choose the appropriate unit system.

The Schrödinger equation

$$\left(-\frac{\hbar^2}{m}\partial_x^2 + V(x) - E\right)\psi(x) = 0.$$

for the neutron-proton system can be transformed into the form

$$\left(-\partial_x^2 + \widetilde{V}(x) - \widetilde{E}\right)\psi(x) = 0$$

where

$$\widetilde{V}(x) = \frac{\hbar^2}{m}V(x)$$

$$\widetilde{E} = \frac{\hbar^2}{m}E.$$

Here $\frac{\hbar^2}{m} = 41.47\text{fm}^2\text{MeV}$.

As we set $x = \rho\cos\theta$ in polar coordinates and ρ is the parameter, we can consider the dynamics of the potential $V(\rho\cos\theta)$ on the interval $[0,\ \pi/2]$ with variation of ρ.

As $\rho \to \infty$ the support of $V(\rho\cos\theta)$ becomes smaller and localizes near $\pi/2$.

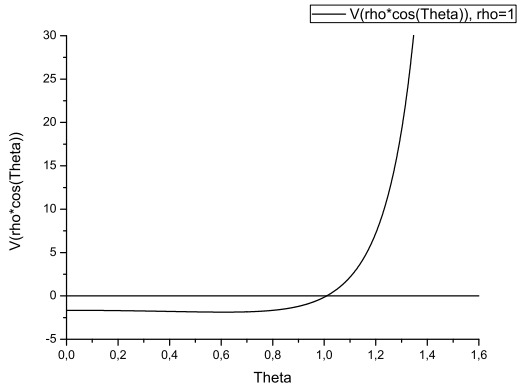

Figure 2. The dynamics of the Malfliet-Tjon potential, $\rho = 1$

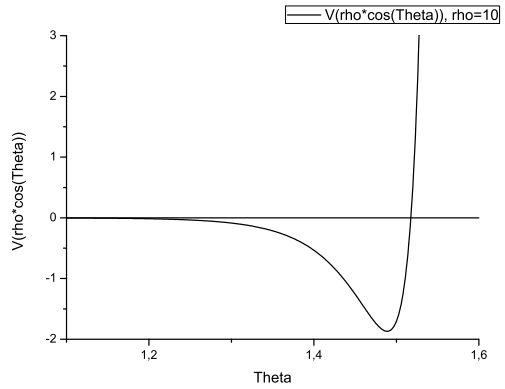

Figure 3. The dynamics of the Malfliet-Tjon potential, $\rho = 10$

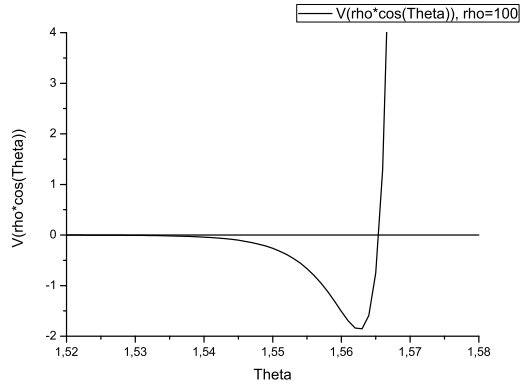

Figure 4. The dynamics of the Malfliet-Tjon potential, $\rho = 100$

7 Numerical calculations

We use the simplest discretisation of the equation, namely, the finite-difference approach, although more sophisticated approaches may be applied in the same manner.

We introduce two dimensional uniformly spaced polar grid with nodes ρ_i, θ_l, $1 \leq i \leq N_\rho, 1 \leq l \leq N_\theta$. The uniformity means that $\rho_{i+1} - \rho_i = \tau$ and $\theta_{l+1} - \theta_l = h$ and τ and h do not depend on numbers i and l.

The discretised equation takes the form

$$\frac{-\phi_k(\theta - h) + 2\phi_k(\theta) - \phi_k(\theta + h)}{\rho^2 h^2} + V(\rho\cos\theta)\phi_k(\theta) = \lambda_k \phi_k(\theta).$$

where k is the number of eigenvalue and eigenfunction. We use zero boundary conditions

$$\phi_k(0) = \phi_k(\pi/2) = 0.$$

For numerical computations we use the Intel® Math Kernel Library 10.0.1 for Unix. It provides us with functions and procedures for the matrix calculations and different linear algebra problems such as eigenfunctions and eigenvalues. This library is highly efficient and optimized.

Particularly we use procedure 'DSTEVX' which computes selected eigenvalues and, optionally, eigenvectors of a real symmetric tridiagonal matrix. Eigenvalues and eigenvectors can be selected by specifying either a range of values or a range of indices. We choose second option and compute both eigenvalues and eigenfunctions with numbers from 0 to 20.

8 Eigenvalues

We estimate the asymptotic behavior and few correction terms in the formalism of the perturbation theory. The asymptotic behavior for eigenvalues λ_k, $k \geq 1$ is

$$\lambda_k(\rho) \sim \left(\frac{2k}{\rho}\right)^2$$

and the first order correction term depends on parameter ρ as $\lambda_k^{(1)} \sim \rho^{-3}$.

We obtain the next results for eigenvalues. The first eigenvalue λ_0's behavior has the form shown in the Fig. 5. As $\rho \to \infty$ the λ_0 becomes the constant value $-0,0538\,\mathrm{fm}^{-2}$ or $-2,2307\,\mathrm{MeV}$.

Few other eigenvalues λ_k, $k \geq 1$ are presented in the Fig. 6.

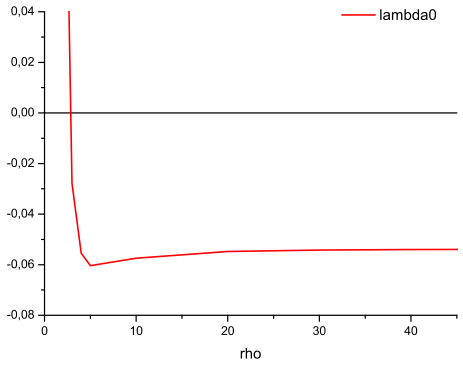

Figure 5. Eigenvalue λ_0

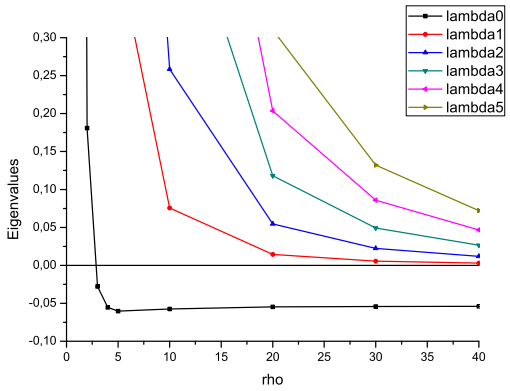

Figure 6. Eigenvalues $\lambda_0 - \lambda_5$

The numerically calculated behavior of eigenvalues is very close to predicted asymptotics. We consider the deviation between calculated eigenvalues and asymptotics and obtain the "asymptotic" region in ρ for which $\lambda_k \sim \lambda_k^{as}$.

- $\rho \sim 10$ – The deviation is significant and varies from 10% up to 90%.
- $\rho \sim 100$ – The deviation is about $5 - 7\%$
- $\rho = 700$ – The deviation is less than 1%
- $\rho \sim 1000$ – The deviation is about $0,7\%$

We conclude that the eigenvalues reach the asymptotic behavior as $\rho \geq 1000$. In the Fig. 7 both numerically calculated eigenvalue λ_{10} and its asymptotic are presented.

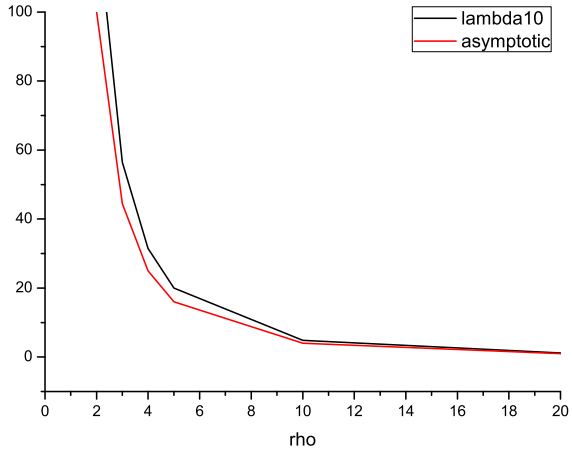

Figure 7. Eigenvalue λ_{10} and its asymptotic behavior

9 Eigenfunctions

We start with the special eigenfunction ϕ_0 which behavior is very different from the other eigenfunctions.

With growth of ρ the support (the interval where the eigenfunction is nonzero) of ϕ_0 decreases, while the peak value increases to infinity. As $\rho \to \infty$ the eigenfunction ϕ_0 transforms into δ-function. This fact leads to a number of computational problems. We have to set step h of the discretisation smaller with grows of ρ in order to keep the accuracy.

The step-by-step transformation of ϕ_0 into δ-function is presented in the Fig. 8

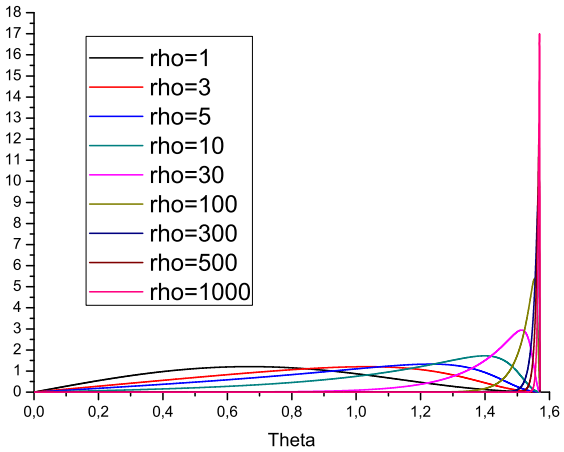

Figure 8. The dynamics of the eigenfunction ϕ_0

or more detailed

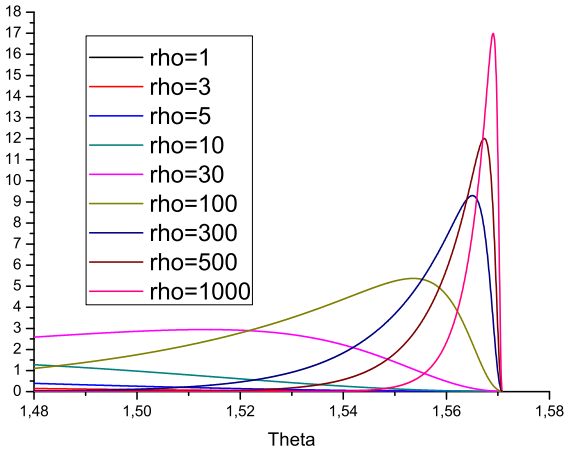

Figure 9. The dynamics of the eigenfunction ϕ_0 near point $\pi/2$

Let us consider the asymptotic behavior of ϕ_k, $k \geq 1$. The dynamics of eigenfunctions with growth of the parameter ρ is presented in next figures.

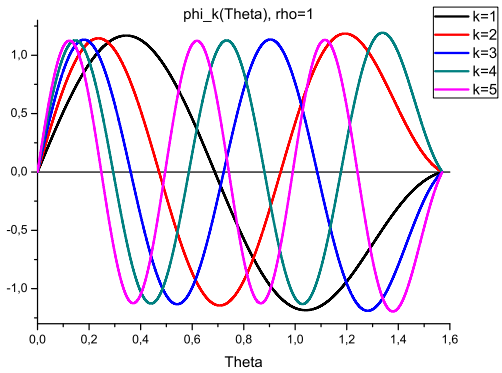

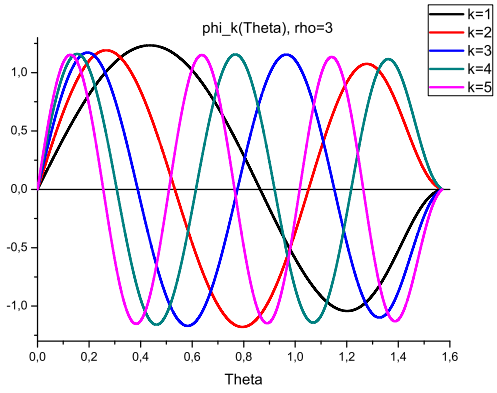

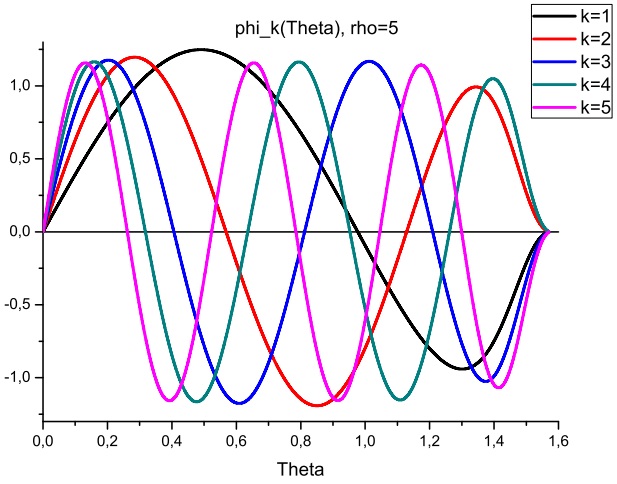
phi_k(Theta), rho=5
k=1
k=2
k=3
k=4
k=5
1,0
0,5
0,0
-0,5
-1,0
0,0
0,2
0,4
0,6
0,8
1,0
1,2
1,4
1,6
Theta

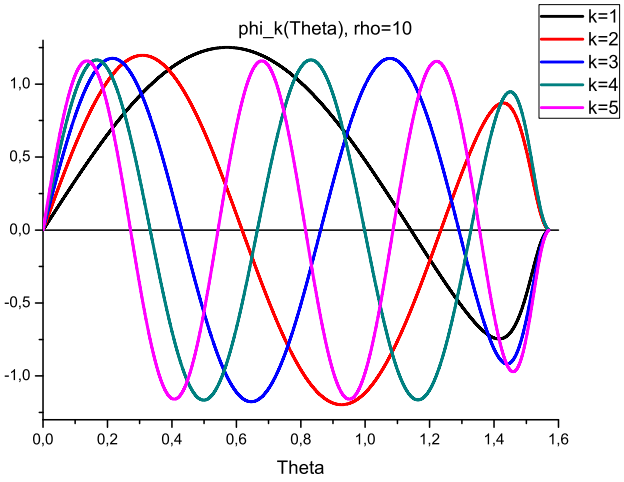
phi_k(Theta), rho=10
k=1
k=2
k=3
k=4
k=5
1,0
0,5
0,0
-0,5
-1,0
0,0
0,2
0,4
0,6
0,8
1,0
1,2
1,4
1,6
Theta

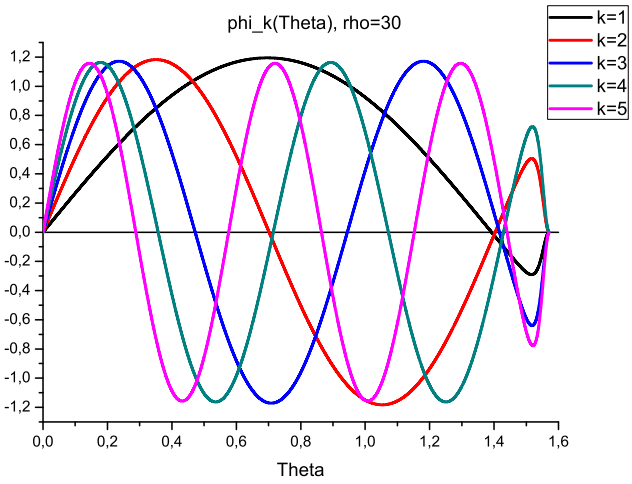
phi_k(Theta), rho=30
k=1
k=2
k=3
k=4
k=5
1,2
1,0
0,8
0,6
0,4
0,2
0,0
-0,2
-0,4
-0,6
-0,8
-1,0
-1,2
0,0
0,2
0,4
0,6
0,8
1,0
1,2
1,4
1,6
Theta

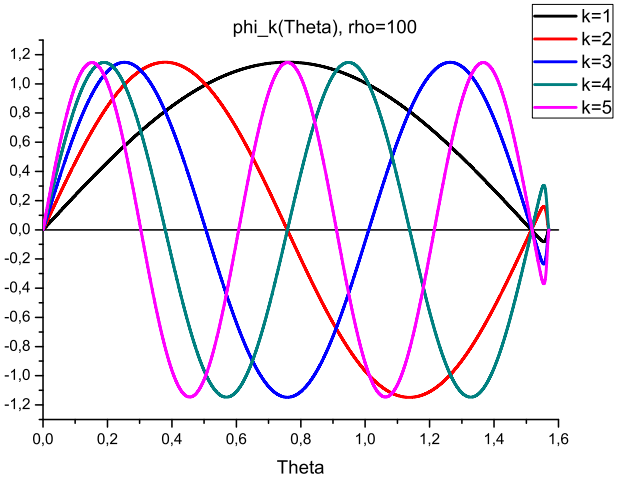
phi_k(Theta), rho=100
k=1
k=2
k=3
k=4
k=5
1,2
1,0
0,8
0,6
0,4
0,2
0,0
-0,2
-0,4
-0,6
-0,8
-1,0
-1,2
0,0
0,2
0,4
0,6
0,8
1,0
1,2
1,4
1,6
Theta

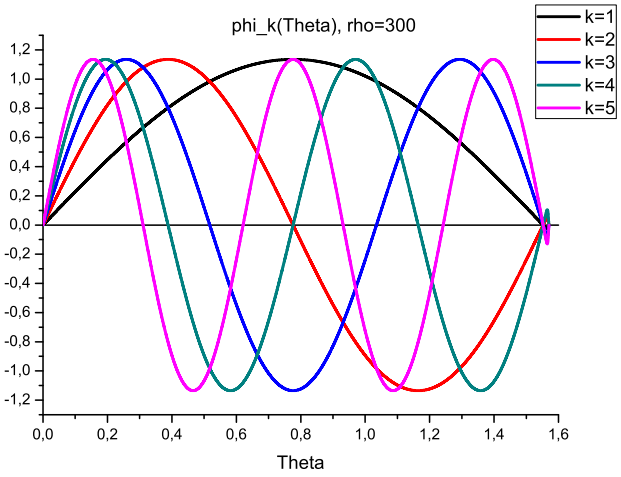
phi_k(Theta), rho=300
k=1
k=2
k=3
k=4
k=5
1,2
1,0
0,8
0,6
0,4
0,2
0,0
-0,2
-0,4
-0,6
-0,8
-1,0
-1,2
0,0
0,2
0,4
0,6
0,8
1,0
1,2
1,4
1,6
Theta

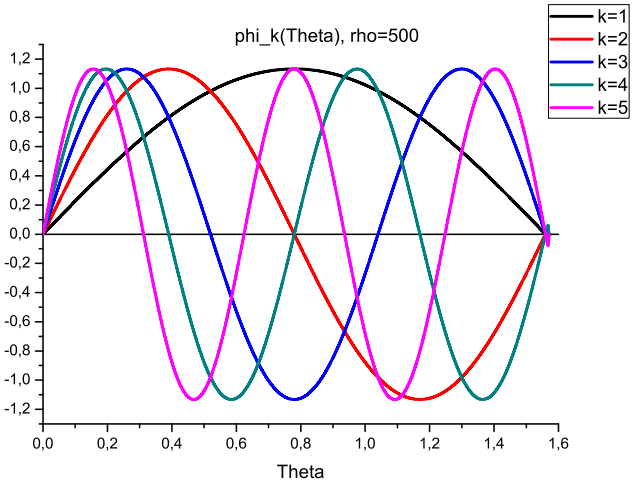
phi_k(Theta), rho=500
k=1
k=2
k=3
k=4
k=5
1,2
1,0
0,8
0,6
0,4
0,2
0,0
-0,2
-0,4
-0,6
-0,8
-1,0
-1,2
0,0
0,2
0,4
0,6
0,8
1,0
1,2
1,4
1,6
Theta

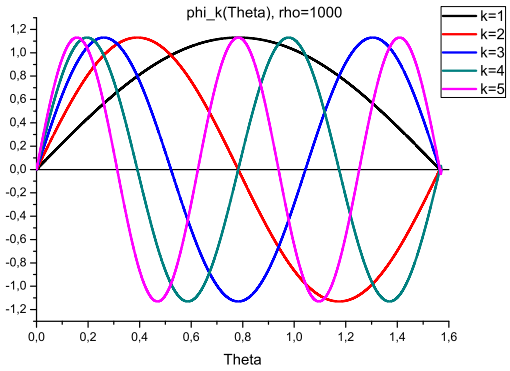

The dynamics of $\phi_1(\theta)$ is shown step-by-step in the Fig. 10. As $\rho \to \infty$ the eigenfunction turns into the asymptotic sin-function.

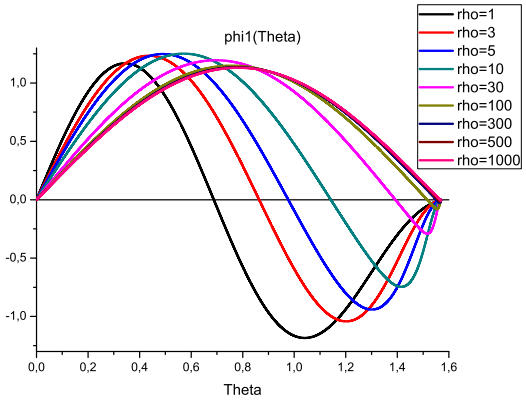

Figure 10. The dynamics of eigenfunction $\phi_1(\theta)$

On the each step we check the orthogonality of the basis. Few matrix elements $\langle \phi_k | \, \phi_n \rangle$ are presented in Tabs. 1, 2. Similar results were obtained for all eigenfunctions.

For $\rho = 100$:

Table 1. The orthogonality of basis functions, $\rho = 100$

	ϕ_0	ϕ_1	ϕ_2	ϕ_3
ϕ_0	$1,000000000000001$	$-0,000000000000000$	$0,000000000000000$	$-0,000000000000000$
ϕ_1	$-0,000000000000000$	$1,000000000000007$	$0,000000000000002$	$-0,000000000000001$
ϕ_2	$0,000000000000000$	$0,000000000000002$	$1,000000000000002$	$0,000000000000000$
ϕ_3	$-0,000000000000000$	$-0,000000000000001$	$0,000000000000000$	$1,000000000000004$

For $\rho = 1000$:

Table 2. The orthogonality of basis functions, $\rho = 1000$

	ϕ_0	ϕ_1	ϕ_2	ϕ_3
ϕ_0	$1,000000000000000$	$-0,000000000000000$	$0,000000000000000$	$0,000000000000000$
ϕ_1	$-0,000000000000000$	$0,999999999999997$	$0,000000000000001$	$-0,000000000000000$
ϕ_2	$0,000000000000000$	$0,000000000000001$	$0,999999999999996$	$-0,000000000000002$
ϕ_3	$0,000000000000000$	$-0,000000000000000$	$-0,000000000000002$	1.000000000000002

As $\rho \to \infty$ calculated eigenfunctions have similar behavior to $\sin(2k\theta)$, but with the small addition in the area near point $\pi/2$. To estimate this addition we calculate the maximum deviation for different values of ρ by the formula

$$\max_{\theta} |\phi_{k,\rho}(\theta) - \sin(2k\theta)|.$$

The significant deviations are observed only near point $\pi/2$. They decrease as $\rho \to \infty$. The absolute deviations are shown on figures 11, 12.

- $\rho = 500$

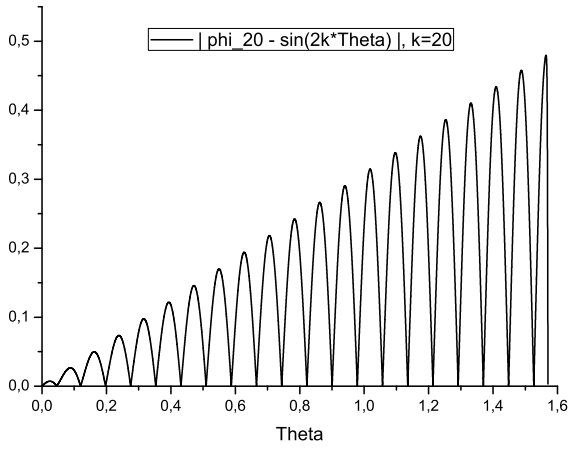

Figure 11. The absolute deviation in case ϕ_{20}, $\rho = 500$

- $\rho = 1000$

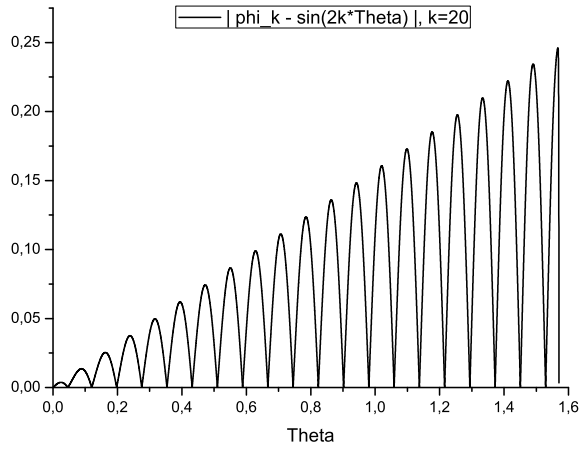

Figure 12. The absolute deviation in case ϕ_{20}, $\rho = 1000$

10 Geometrical connections

We introduce the off-diagonal matrix of the geometrical connection A with elements

$$A_{ki}(\rho) = \langle \phi_k |\, \phi_i' \rangle = \int_0^{\pi/2} d\theta\, \phi_k^*(\theta|\,\rho) \frac{\partial \phi_i(\theta|\,\rho)}{\partial \rho}.$$

These elements are presented in the equation

$$\left(-\partial_\rho^2 - \frac{1}{4\rho^2} + \Lambda(\rho) - E\right) G = \left(-A'(\rho) - A^2(\rho) + B(\rho) - W(\rho)\right) G \tag{10.24}$$

and determine the behavior of the right hand side as $\rho \to \infty$. The potential terms in the left hand side of the equation decreases as ρ^{-2}. If the right hand side decreases faster, it can be neglected. The solution in this case is known and can be used as the boundary condition for full equation.

The potential formula for elements A_{ki} is

$$A_{ki} = \frac{\langle \phi_k |\, \partial_\rho (\rho^2 V(\rho\cos\theta))|\, \phi_i \rangle}{\rho^2(\lambda_i - \lambda_k)}.$$

The diagonal element A_{kk} is equal to 0 and $A_{ki} = -A_{ik}$. We separate the behavior of A_{k0} and A_{ki} because of its different dependence on the parameter ρ.

- Geometrical connection A_{ki} with $k = 0$ or $i = 0$. It differs from the other elements, because $\lambda_0 = \epsilon = const$ as $\rho \to \infty$. From analytical calculations we estimate its behavior as

  $$A_{ki} \sim \rho^{-5/2}.$$

  Results from numerical calculation are shown on the Fig. 13.

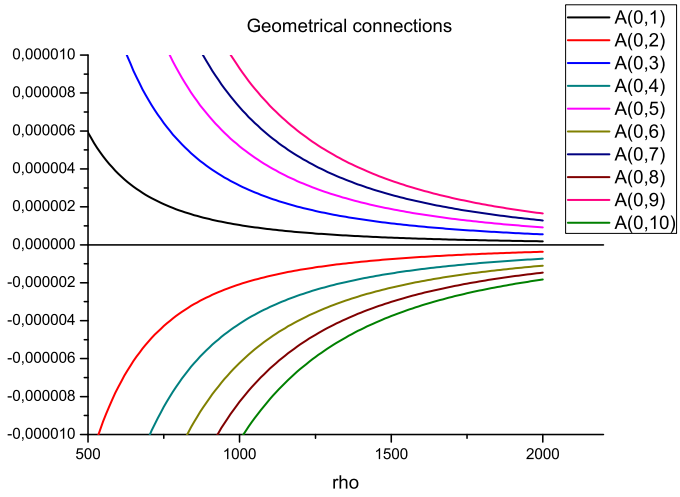

Figure 13. Geometrical connections A_{0k}, $k = 1, \ldots, 10$

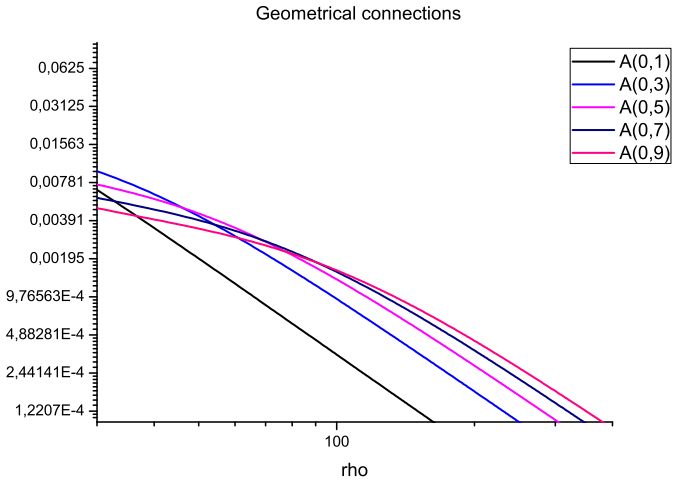

Figure 14. Geometrical connections A_{0k} in double logarithmic scale

We plot this graphs in the double logarithmic scale (Fig. 14). The intercept coefficient in asymptotic linear area is slightly smaller than $-2,5$.

- Geometrical connection A_{ki} with $k, i \neq 0$. We estimated its behavior as

$$A_{ki} \sim \rho^{-2}.$$

Results from numerical calculation are shown on the figures 15, 16.

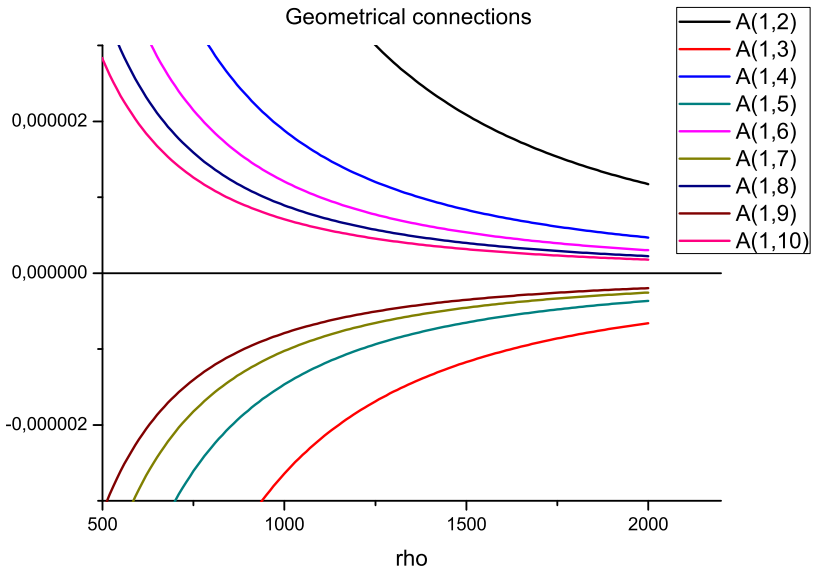

Figure 15. Geometrical connections A_{1k}, $k = 2, \ldots, 10$

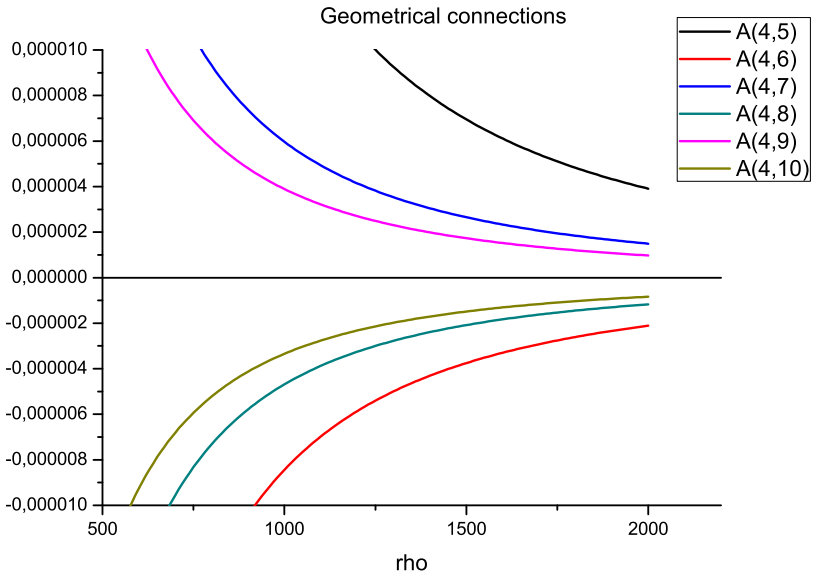

Figure 16. Geometrical connections A_{4k}, $k = 5, \ldots, 10$

We plot this graphs in the double logarithm scale (Fig. 17). The intercept coefficient in asymptotic linear area is slightly smaller than -2.

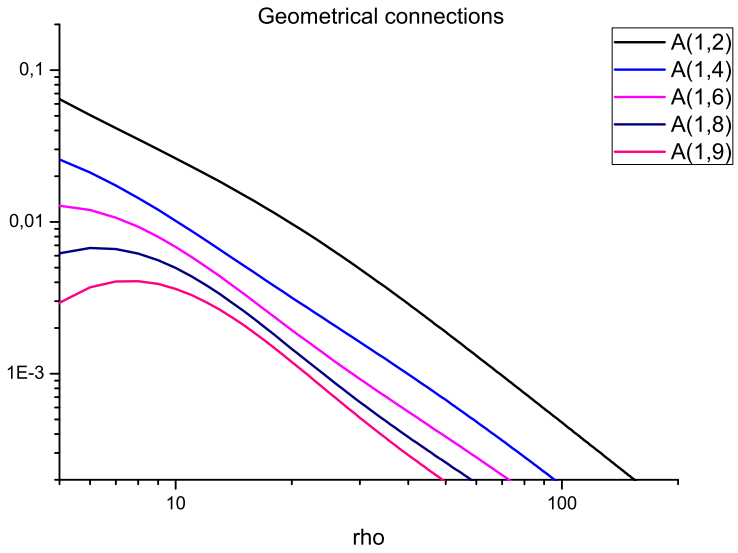

Figure 17. Geometrical connections A_{1k} in double logarithmic scale

11 Conclusions

We choose basis functions ϕ_k and study their properties, particularly eigenvalues λ_k and geometrical connections A_{ij}. We estimate asymptotics and compare them with numerically calculated values. Results are in good agreement with each other.
The behavior of geometrical connections A_{ij} is regular in case of the Malfliet-Tjon potential. Obtained results lead us to the conclusion that the right hand side of the equation (5.19) tends to 0 faster than the left hand side as $\rho \to \infty$ and can be neglected in asymptotic region.

Acknowledgements

I would like to thank Prof. Dr. S.L. Yakovlev.

References

[1] Faddeev L.D., Merkuriev S.P. *Quantum Scattering Theory for Several Particle Systems*